Electronic Supplementary Information

Rapid Detection Strategies for the Ultra-level Chemosensing of Uranyl Ions

Selva Kumar R[a,b], Vetriarasu V[a], R. Bhaskar[a], S.K. Ashok Kumar[a]*, Kari Vijayakrishna[c], Akella Sivaramakrishna[a], C.V.S. Brahmmananda Rao[d], N. Sivaraman[d], and Suban K. Sahoo[e]

[a] Department of Chemistry, School of Advanced Sciences, Vellore Institute of Technology, Vellore-632014, Tamil Nadu, India.

[b] Department of Chemistry, Saveetha School of Engineering, Saveetha Institute of Medical and Technological Sciences, (SIMATS), Chennai- 602105, Tamil Nadu, India.

[c] School of Basic Sciences, Indian Institute of Technology Bhubaneswar, Bhubaneshwar, Odisha 752050, India.

[d] Indira Gandhi Centre for Atomic Research, HBNI, Kalpakkam-603102, Tamil Nadu, India.

[e] Department of Chemistry, Sardar Vallabhbhai National Institute Technology, Surat-395007, Gujarat, India.

† E-mail: ashok312002@gmail.com.

Contents

Colour Space and its Conversion

Conversion of smartphone camera image dada into the CIE 1931 colour space involves three steps. In which the colour space terms are derived from the conventional RGB values.

At first, the non-linear RGB values are obtained from smartphone must be converted into linear RGB values using the following equations.

$$R_l = (0.055 + R_c / 1.055)^{2.4} \quad \text{----- (1)}$$

$$G_l = (0.055 + G_c / 1.055)^{2.4} \quad \text{----- (2)}$$

$$B_l = (0.055 + B_c / 1.055)^{2.4} \quad \text{----- (3)}$$

Next, the linear RGB values are converted into tristimulus values X, Y, Z by the following relationships.

$$\begin{bmatrix} X \\ Y \\ Z \end{bmatrix} = \begin{bmatrix} 0.607 & 0.174 & 0.200 \\ 0.299 & 0.587 & 0.114 \\ 0.000 & 0.066 & 1.116 \end{bmatrix} \begin{bmatrix} R_l \\ G_l \\ B_l \end{bmatrix} \text{----- (4)}$$

Finally, the X, Y, Z tristimulus values are converted into 2-D (x,y) CIE 1931 chromaticity space using the following relationships.

$$x_j = \frac{X}{X + Y + Z} \text{----- (5)}$$

$$y_j = \frac{Y}{X + Y + Z} \text{----- (6)}$$

The new colour space specified by x, y and Y is represented in 2-D chromaticity diagram. The pure colour is located in boundary curve from blue (380 nm) to red (700 nm), while all the mixed colours are represented within the area enclosed by the curve.

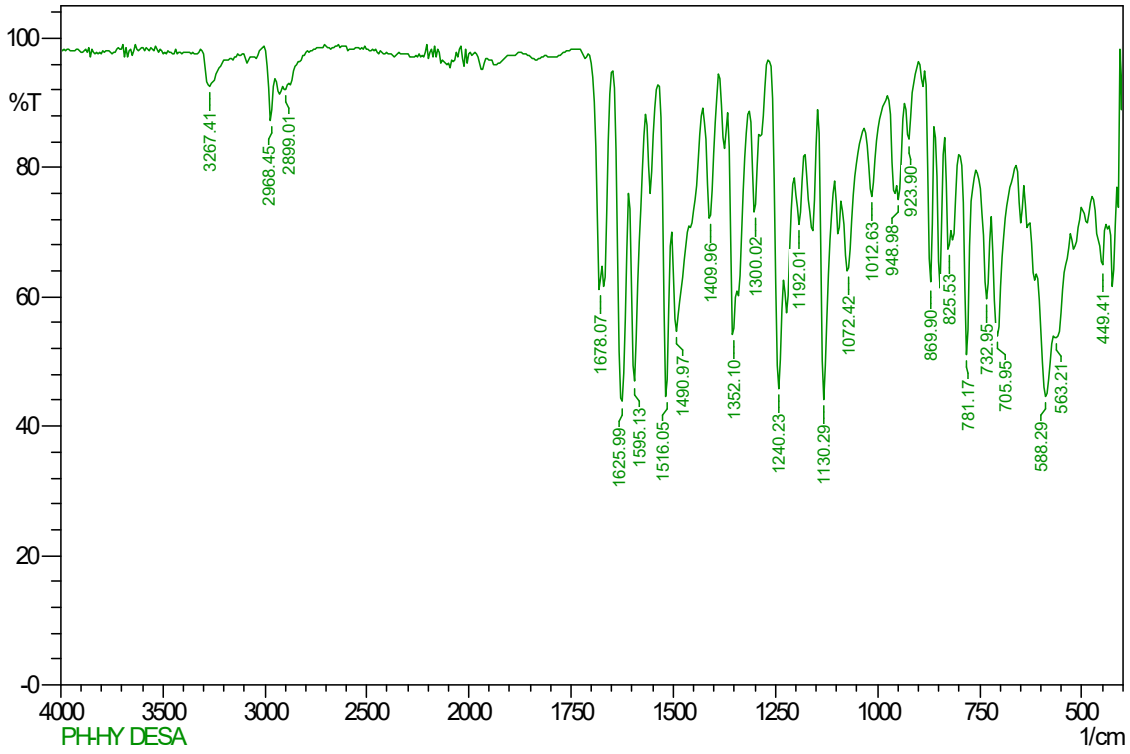

Figure 1S. FTIR spectrum of **L**

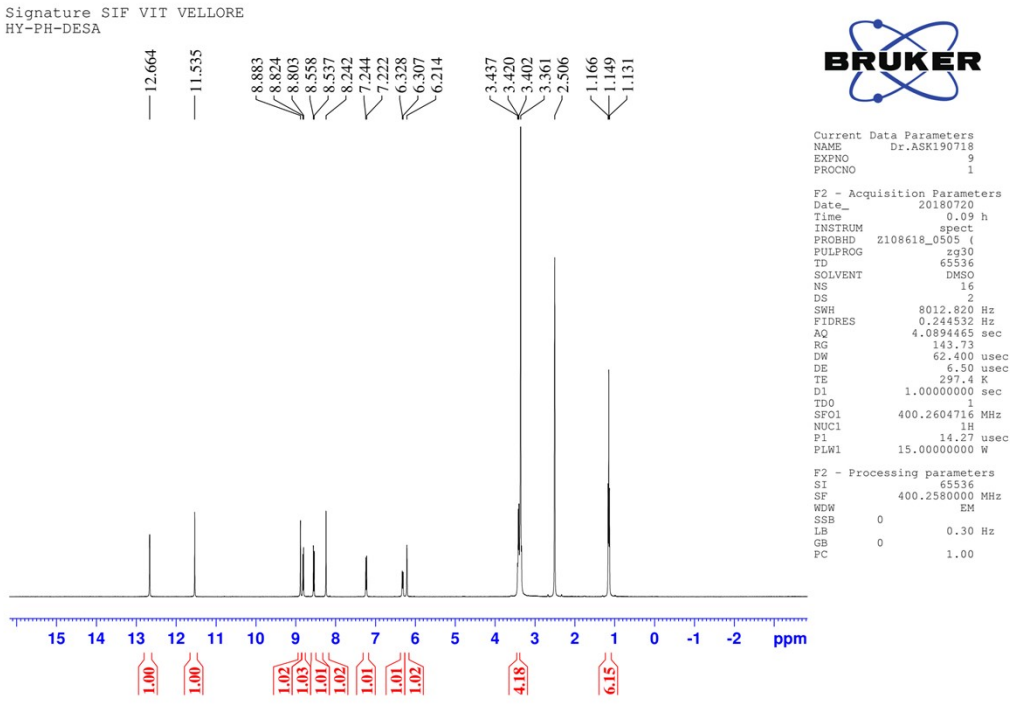

Figure 2S. ^{1}H NMR spectrum of **L**

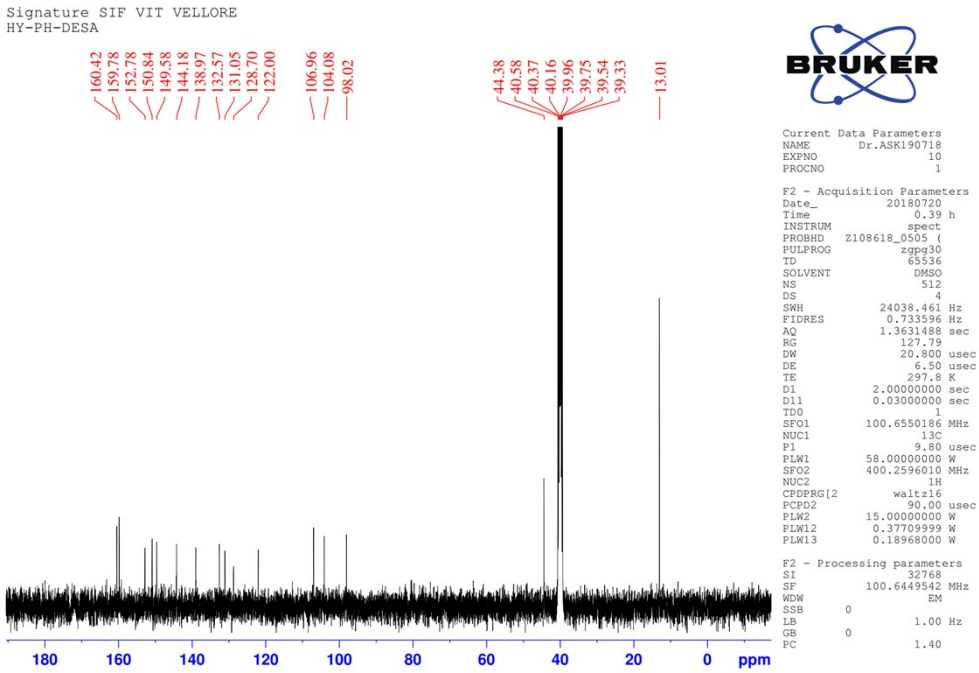

Figure 3S. ^{13}C NMR spectrum of **L**

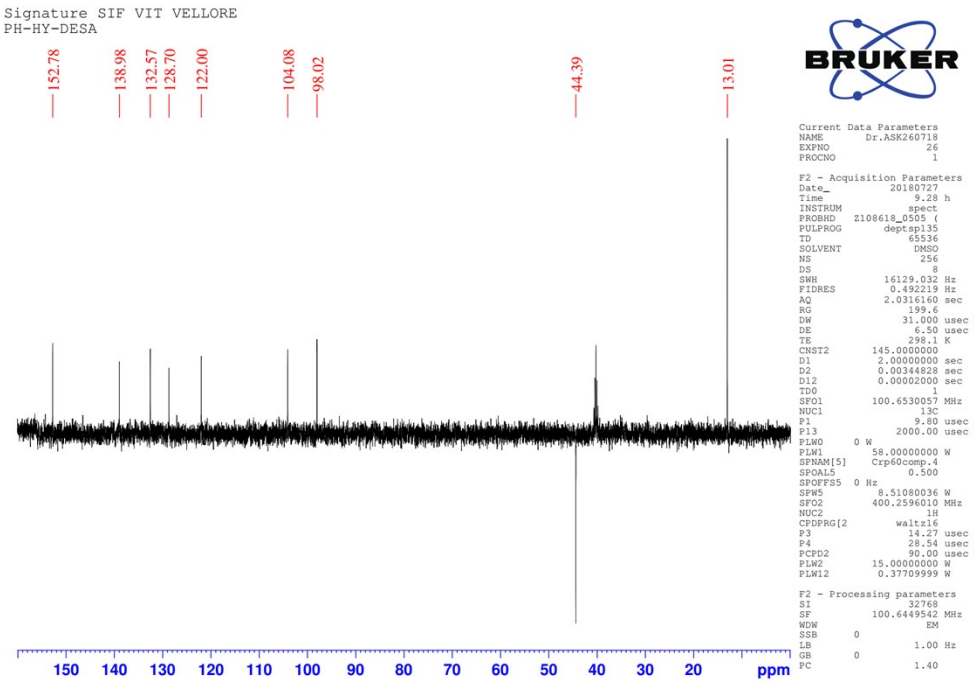

Figure 4S. DEPT-135 NMR spectrum of **L**

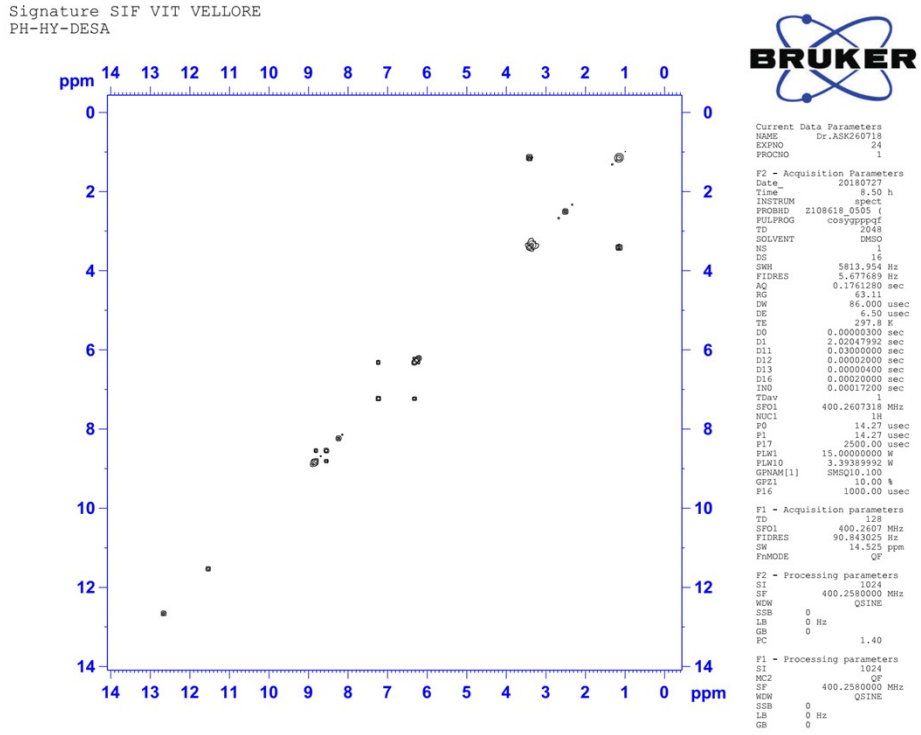

Figure 5S. HH-COSY NMR spectrum of **L**

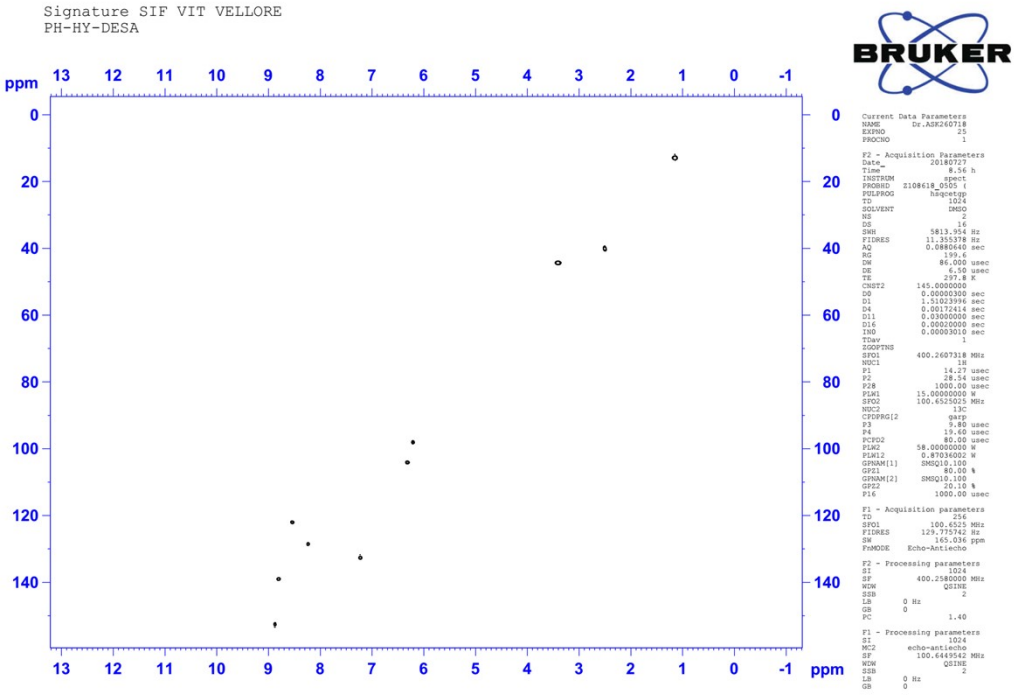

Figure 6S. CH-COSY NMR spectrum of **L**

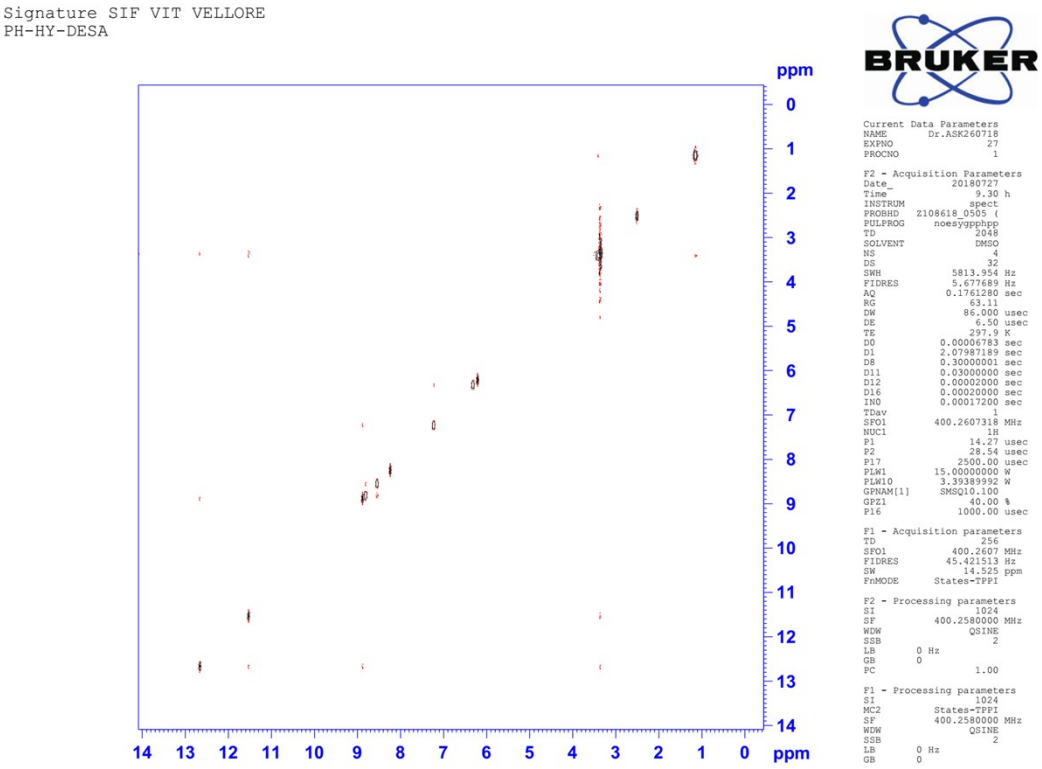

Figure 7S. NOESY NMR spectrum of **L**

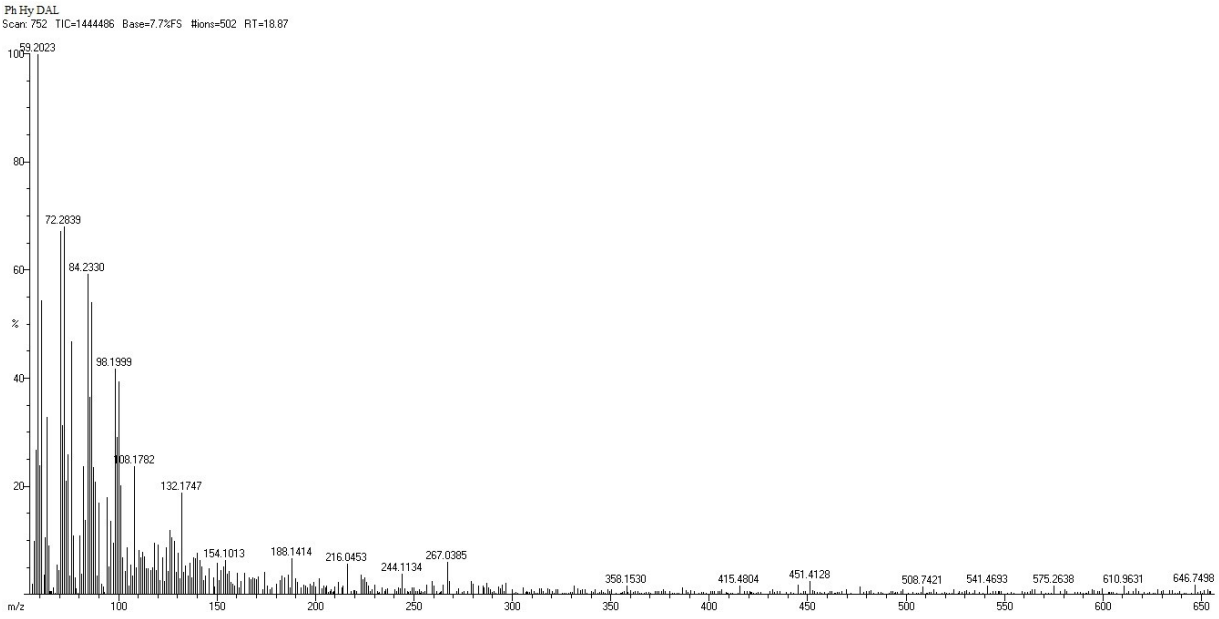

Figure 8S. HR-Mass spectrum for **L**

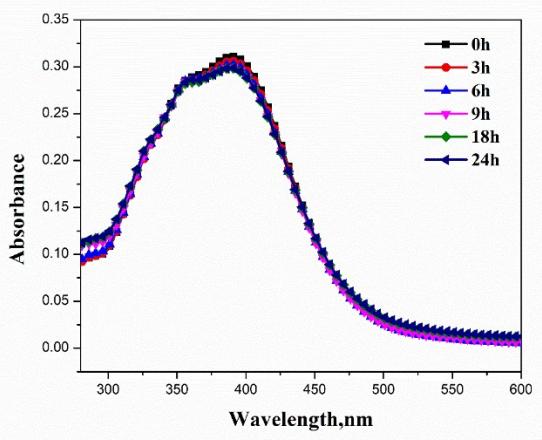

Figure 9S. Stability examination of **L** in DMSO in (8:2, v/v) DMSO:water media

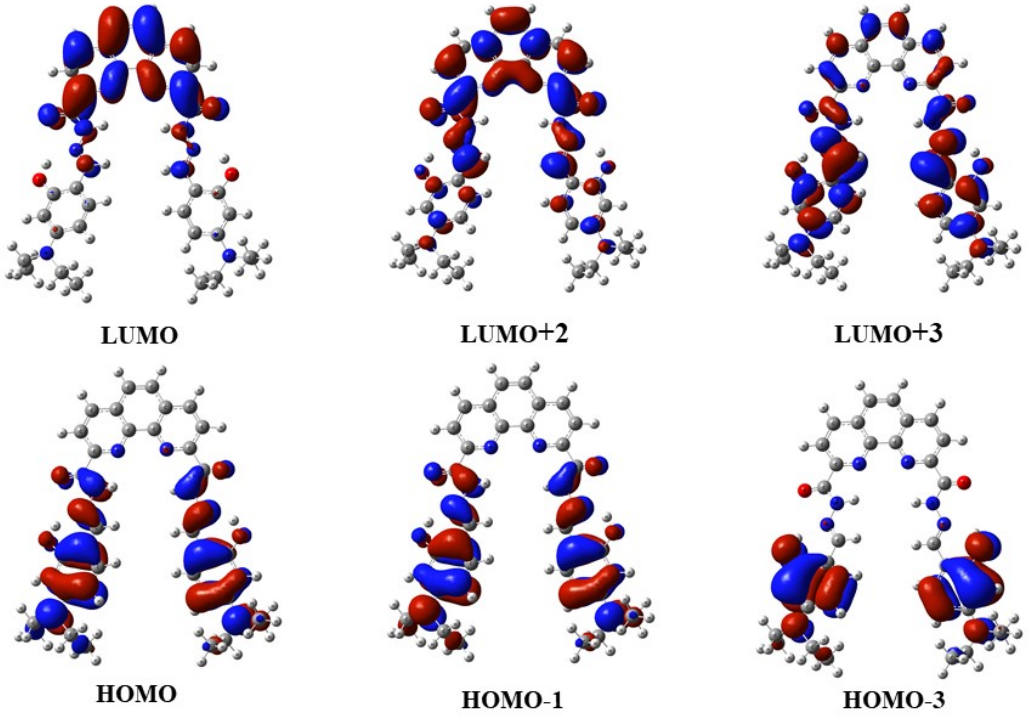

Figure 10S. FMO of **L** by TDDFT analysis.

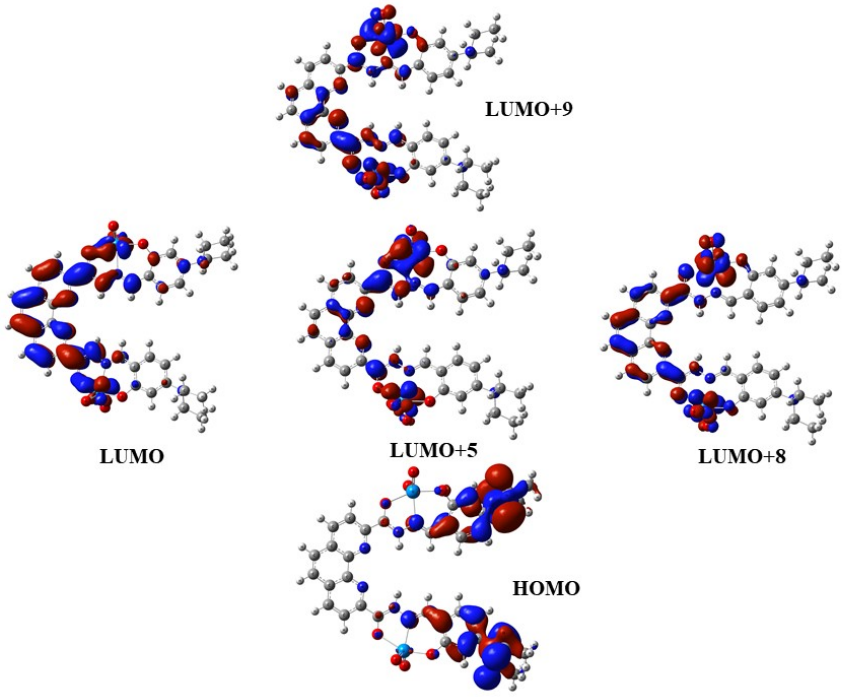

Figure 11S. FMO of **L**-UO_2^{2+} complex by TDDFT analysis.

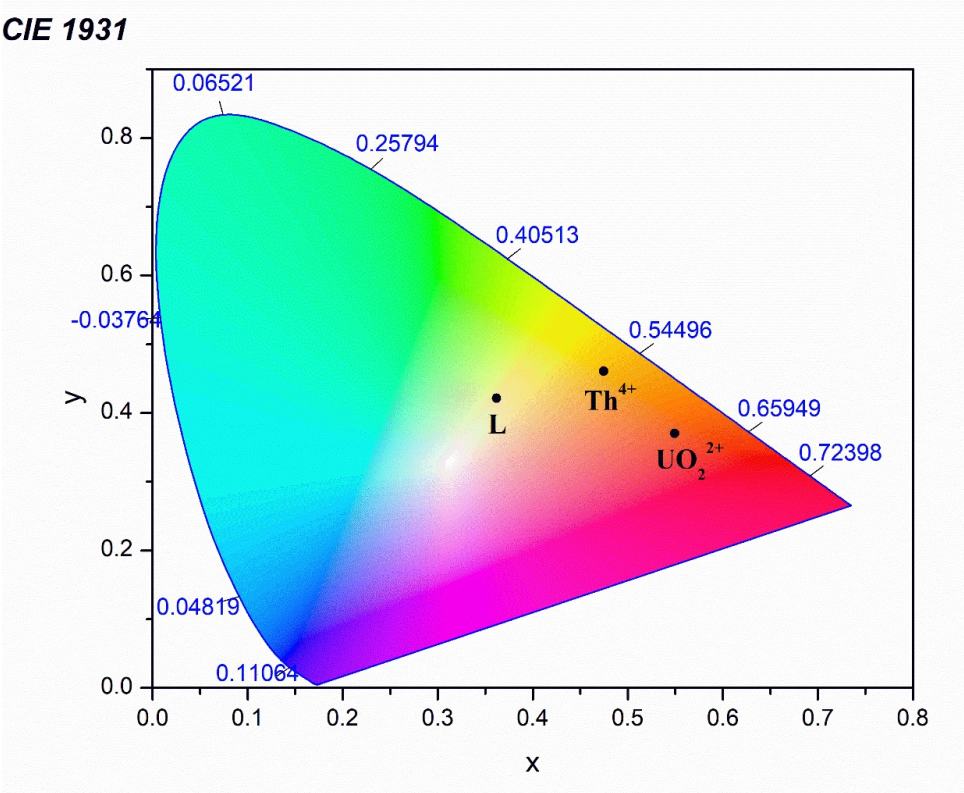

Figure 12S. Colour change of **L** with Th^{4+} and UO_2^{2+} in CIE 1931 colour space

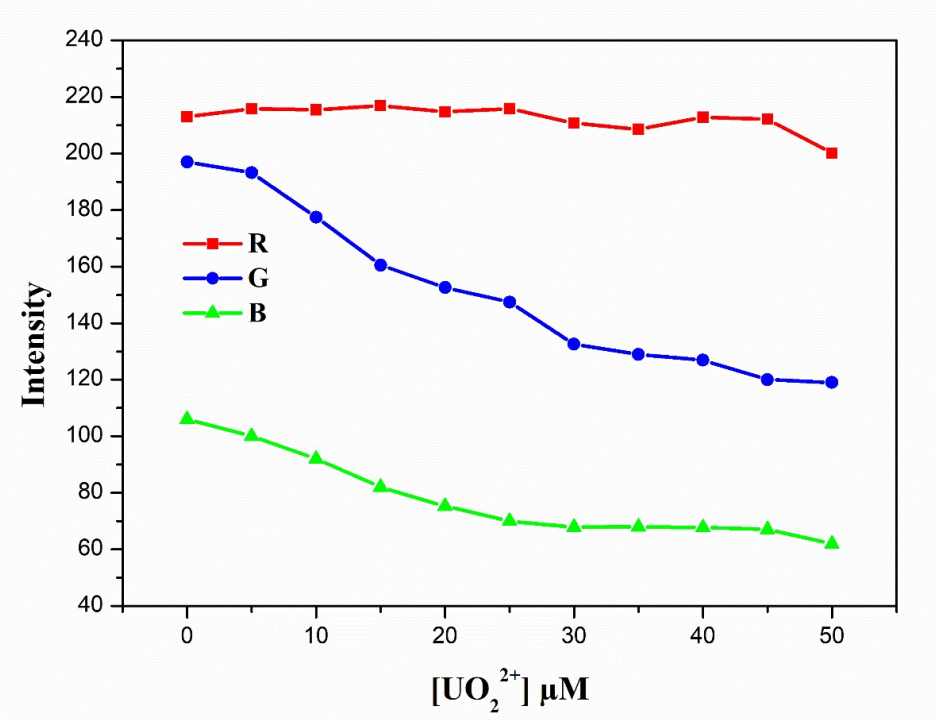

Figure 13S. Change in RGB values of **L** with respect to UO_2^{2+} concentration.

Table 1S. The atomic charges on selected atoms

Atom	L		L-UO_2^{2+}	
	Mullikan charge	**NBO charge**	**Mullikan charge**	**NBO charge**
C=O	-0.336	-0.591	-0.570	-0.633
Imine-N	-0.283	-0.334	-0.484	-0.425
Nap-OH	-0.384	-0.690	-0.603	-0.641
U	-	-	1.637	1.877

Table 2S. UV-vis spectra characteristic by experimental and theoretical.

	Experimental		**Theoretical**			
	λ_{max} (nm)	ε ($L\ M^{-1}cm^{-1}$)	Excitation energy (nm)	Oscillator strength	Excited state	Key transitions
L	353	47460	329.29	0.5454	$S_0 \rightarrow S_{13}$	H-1 → L+3 (89%)
	389	50500	388.96	0.3238	$S_0 \rightarrow S_6$	H → L+2 (71%), H-3 → L (27%)
L-UO_2^{2+}	482	55275	488.24	0.0538	$S_0 \rightarrow S_{25}$	H → L+8 (65%), H → L+9 (20%), H→L+5 (2%)

*H- HOMO, L-LUMO

Table 3S. Comparison of the sensing ability of **L** towards UO_2^{2+} determination with previously reported work.

Sensors	UV-Vis	Test Strip	RGB	LOD	pH	Solvent media used	Interference
DNAzyme-functionalized magnetic beads-AuNP [54]	Yes	NR	NR	74 pM	7.5	TMB-H_2O_2	Fe^{3+}, Ni^{2+}
DNAzyme modulator[55]	Yes	NR	NR	2 nM	3.5	TMB-H_2O_2	Mn^{2+}, Al^{3+}
DNAzyme-functionalized magnetic beads[56]	Yes	NR	NR	0.33 nM	7.5	TMB-H_2O_2	Mg^{2+}, Mn^{2+}, Th^{4+}, La^{3+}
Terbium (III)-based MOF [57]	Yes	NR	NR	0.9 µg/L	4.0	H_2O-suspension	NR
Quinoxolinol Salen [58]	Yes	NR	NR	1.9 µM	NR	DMF:H_2O (8:2, v/v)	Cu^{2+}, Ni^{2+}
O-phosphoryl ethanolamine-functionalized gold nanoparticles [59]	Yes	NR	NR	0.084 µM	4.0	H_2O-suspension	Co^{2+}
2-(5-Bromo-2-pyridylazo)-5-(diethylamino) phenol in CTA nana fiber [60]	Yes	Yes	Yes	0.185 µM	6.0	Solid Phase	Fe^{2+}, Cu^{2+}
This work (L)	Yes	Yes	Yes	73 nM	2-10	DMSO:H_2O (8:2, v/v)	No interference

NR= not reported, TMB - 3,3',5,5'-tetramethylbenzidine sulfate,

****